0013-7227/01/$03.00/0
Printed in U.S.A.

Endocrinology 142(10):4401–4413

Calcitonin (CT) Rapidly Increases Na^+/H^+ Exchange and Metabolic Acid Production: Effects Mediated Selectively by the C1a CT Receptor Isoform

ANU SANTHANAGOPAL, PETER CHIDIAC, WILLIAM C. HORNE, ROLAND BARON, AND S. JEFFREY DIXON

CIHR Group in Skeletal Remodeling, Department of Physiology, Division of Oral Biology (A.S., S.J.D.), and Department of Pharmacology & Toxicology (P.C.), Faculty of Medicine & Dentistry, The University of Western Ontario, London, Canada N6A 5C1; and Departments of Cell Biology and Orthopedics and the Yale Cancer Center (W.C.H., R.B.), Yale University School of Medicine, New Haven, Connecticut 06520

Two isoforms of the calcitonin receptor are expressed in rabbit: the common C1a isoform and the calcitonin receptor Δe13 isoform, which has a deletion in the seventh transmembrane domain. Using microphysiometry, we investigated the effects of calcitonin on proton efflux from HEK293 cells stably transfected with C1a, calcitonin receptor Δe13, or empty vector. In C1a-expressing cells only, calcitonin rapidly induced a biphasic elevation in proton efflux consisting of an initial transient and a sustained plateau, accompanied by an increase in lactate efflux. Inhibitors of Na^+/H^+ exchange abolished only the initial transient, whereas removal of extracellular glucose abolished only the sustained plateau. These data suggest that activation of Na^+/H^+ exchange mediates the initial transient, whereas increased glucose metabolism underlies the sustained plateau. Because both receptor isoforms activate adenylyl cyclase, the lack of effect of calcitonin on proton efflux from calcitonin receptor Δe13-expressing cells argued against involvement of cAMP in activating proton efflux. Similarly, studies involving elevation or buffering of cytosolic free Ca^{2+} concentration argued against involvement of Ca^{2+}. Activation of PKC mimicked the plateau phase of calcitonin-induced proton efflux from C1a cells, whereas inhibition or depletion of PKC suppressed it. Activation of proton transport and production are novel cellular responses to calcitonin, mediated selectively by the C1a receptor isoform via a mechanism involving PKC. (*Endocrinology* 142: 4401–4413, 2001)

CALCITONIN (CT) IS a 32-amino acid hormone synthesized and secreted by the parafollicular cells of the thyroid gland. CT acts primarily on bone and kidney to reduce plasma Ca^{2+} levels by inhibiting bone resorption and promoting Ca^{2+} excretion. Therefore, CT is administered therapeutically in the treatment of diseases characterized by high bone turnover, including Paget's disease of bone, malignancy-associated hypercalcemia, and osteoporosis (1). Mice homozygous for knockout of CALC I (the gene encoding CT and CT gene-related peptide) develop osteopenia, indicating a role for CT in skeletal homeostasis *in vivo* (2).

The CT receptor (CTR), a G protein-coupled receptor, has been identified in a number of tissues, and the existence of splice variants has been reported (3). The most common isoform of the CTR, C1a, was originally cloned from porcine kidney (4) and is also expressed in human, mouse, rat, and rabbit cells (5–10). A novel isoform in rabbit, CTRΔe13, is generated by deletion of exon 13 during mRNA processing, resulting in the absence of 14 amino acid residues in the putative 7th transmembrane spanning domain. This deletion reduces the affinity of the CTRΔe13 isoform for CT. The dissociation constant (K_d) for binding of salmon CT to the CTRΔe13 isoform is 9 nM, whereas the K_d for the C1a isoform is 0.2 nM (10). Both isoforms activate adenylyl cyclase, leading to production of cAMP and activation of PKA. In contrast, only the C1a isoform couples to G_q, activating PLC, which in turn leads to Ca^{2+} mobilization and activation of PKC. It has been suggested that CT-induced elevations in cAMP and cytosolic free Ca^{2+} concentration ($[Ca^{2+}]_i$) have two separate effects on osteoclasts: abolition of cell motility, and induction of cellular retraction, respectively (11). Studies have shown that in addition to G_s and G_q, the C1a isoform couples to G_i, and that the inhibition of adenylyl cyclase by G_i is negatively regulated by PKC (12). The C1a isoform induces Shc phosphorylation and Erk1/2 activation by mechanisms involving G_i, PKC, and cytosolic Ca^{2+} (13).

Expression of C1a and CTRΔe13 isoforms vary in a tissue-specific manner, with CTRΔe13 accounting for less that 15% of the total CTR mRNA in rabbit osteoclasts, kidney, and brain, but comprising at least 50% of the transcripts in skeletal muscle and lung (10). Characterization of the signaling pathways activated by these two receptor isoforms is crucial for understanding the function of these receptors in osteoclasts and other target cells.

G protein-coupled receptors regulate critical intracellular processes such as ion transport and cellular metabolism. Ion transport plays important physiological roles in both bone and kidney, which are key targets for CT. However, little is

Abbreviations: BAPTA-AM, 1,2-Bis-(2-aminophenoxy)ethane-*N,N,N′,N′*-tetraacetic acid tetra(acetoxymethyl)ester; $[Ca^{2+}]_i$, cytosolic free Ca^{2+} concentration; CPT-cAMP, 8-(4-chlorophenylthio)-cAMP; CT, calcitonin; CTR, CT receptor; EC_{50}, concentration required to produce 50% of maximum effect; IBMX, isobutylmethylxanthine; indo-1 AM, indo-1 penta(acetoxymethyl)ester; K_d, dissociation constant; LPA, lysophosphatidic acid; NHE, Na^+/H^+ exchanger; SERCA, sarco-endoplasmic reticulum Ca^{2+}-ATPase; TPA, 13-*O*-tetradecanoyl phorbol-13-acetate.

known about regulation of ion transport and metabolism by the C1a and CTRΔe13 CTR isoforms. The purpose of this study was to determine the effects of CT on proton efflux from human embryonic kidney cells transfected with either the C1a or CTRΔe13 isoform. We examined the ability of CT to modulate proton efflux and investigated underlying mechanisms and signaling pathways. Here, we report novel cellular responses to CT mediated specifically by the C1a receptor isoform.

Materials and Methods

Materials and solutions

α-MEM (catalog no. 12571) buffered with HCO_3^- (26 mM), PBS (catalog no. 14040), FBS (catalog no. 26140), antibiotic solution (penicillin, 10,000 U/ml; streptomycin, 10,000 μg/ml; Amphotericin, 25 μg/ml, catalog no. 15240), trypsin solution (Ca^{2+} and Mg^{2+} free, 0.05% trypsin and 0.53 mM EDTA, catalog no. 25300), G418 (catalog no. 11811), HCO_3^-- and glucose-free DMEM (catalog no. 23800), and HCO_3^--free MEM (catalog no. 41500 and catalog no. 41200) were obtained from Gibco Laboratories (Burlington, Ontario, Canada). Bovine albumin (fraction V, fatty acid free) was from Roche Molecular Biochemicals (Laval, Quebec, Canada; catalog no. 775835). DMEM (catalog no. D-7777), amiloride (catalog no. A-7410), bafilomycin A_1 (catalog no. B-1793), 8-(4-chlorophenylthio)-cAMP (CPT-cAMP) (catalog no. C-3912), isobutylmethylxanthine (IBMX, catalog no. I-5879), and lysophosphatidic acid (1-oleoyl-2-hydroxy-*sn*-glycero-3-phosphate) (LPA) (catalog no. L-7260) were obtained from Sigma (St. Louis, MO). Amiloride and CPT-cAMP were dissolved in standard superfusion medium just before use, whereas IBMX was dissolved in dimethylsulfoxide. Indo-1 penta(acetoxymethyl)ester (indo-1 AM, catalog no. I-1223), 1,2-bis-(2-aminophenoxy)ethane-*N*,*N*,*N*′,*N*′-tetraacetic acid tetra(acetoxymethyl) ester (BAPTA-AM, catalog no. B-6769), and thapsigargin (catalog no. T-7459) were obtained from Molecular Probes, Inc. (Eugene, OR). BAPTA-AM, indo-1 AM, and thapsigargin were dissolved in dimethyl sulfoxide and stored in aliquots at −20 C. Salmon CT was obtained from Bachem (Torrance, CA; catalog no. H-2260) or Rorer Pharmaceutical (Fort Washington, PA). Stock solutions of CT were prepared in 0.2% sodium acetate and 0.05% sodium chloride with 1 mg/ml bovine albumin and stored in aliquots at −80 C. 1-[6-((17β-3-methoxyestra-1,3,5 (10)-trien-17-yl) amino)hexyl]-1H-pyrrole-2,5-dione (U-73122, catalog no. 662035), 1-[6-((17β-3-methoxyestra-1,3,5 (10)-trien-17-yl)amino)hexyl]-2,5-pyrrolidinedione (U-73343 catalog no. 662041), bisindolylmaleimide I (2-[1-(3-dimethylaminopropyl)-1H-indol-3-yl]-3-(1H-indol-3-yl)maleimide, catalog no. 203291), staurosporine (catalog no. 569397), and ionomycin (catalog no. 407952) were obtained from Calbiochem (San Diego, CA); and stock solutions of all these agents were prepared in dimethyl sulfoxide and stored in aliquots at -80 C. Cariporide (HOE 642) was generously provided by Aventis Pharma Deutschland GmbH (Frankfurt am Main, Germany). Cariporide was dissolved in water and stored in aliquots at −20 C. Stock solution of TPA (13-*O*-tetradecanoyl phorbol-13-acetate) was prepared in dimethyl sulfoxide and stored at −20 C. 2-Deoxy-D-[1,2-N-^{3}H]glucose (26 Ci/mmol) was purchased from NEN Live Science Products, Inc. (Boston, MA).

Standard superfusion medium, used in experiments monitoring proton efflux, was HCO_3^--free MEM (catalog no. 41500) supplemented with HEPES (1 mM) and bovine albumin (1 mg/ml) and adjusted to 290 ± 5 milliosmoles/liter with NaCl, and pH 7.30 ± 0.02 with NaOH. Glucose-free superfusion medium was DMEM (catalog no. 23800) without glucose or HCO_3^-, supplemented with HEPES (1 mM), L-glutamine (2 mM), bovine albumin (1 mg/ml), and adjusted to 290 ± 5 milliosmoles/liter and to pH 7.30 ± 0.02. The buffering power of the superfusion solutions was determined over a pH range of 7.0–7.3 at 37 C and found to be 1.4 ± 0.1 mM/pH unit for standard medium and 1.3 ± 0.1 mM/pH unit for glucose-free medium.

For experiments measuring changes in $[Ca^{2+}]_i$, harvested cells were resuspended in HCO_3^--free MEM (catalog no. 41200) supplemented with HEPES (20 mM) adjusted to 290 ± 5 milliosmoles/liter and pH 7.30 ± 0.02. During $[Ca^{2+}]_i$ measurements, cells were placed in continuously stirred Na^+-HEPES buffer (135 mM NaCl, 5 mM KCl, 1 mM $MgCl_2$, 1 mM $CaCl_2$, 10 mM glucose, and 20 mM HEPES, 290 ± 5 milliosmoles/liter, pH 7.30 ± 0.02).

Cells and culture

We used HEK293 cells, which stably express the rabbit CTR isoform C1a (C1a cells), the CTRΔe13 isoform (CTRΔe13 cells), or empty vector (pBK-CMV). CT activates adenylyl cyclase in both C1a cells and CTRΔe13 cells, and the concentrations of CT required to produce half-maximal (EC_{50}) cAMP responses are approximately 0.06 nM and 0.6 nM, respectively. Maximum cAMP responses are similar in both cell types (10). Cells were maintained in DMEM (catalog no. D-7777) supplemented with HCO_3^- (24 mM), heat-inactivated FBS (10% vol/vol), G418 (500 μg/ml), and antibiotic solution (1% vol/vol), pH 7.30 ± 0.02, in 5% CO_2 at 37 C. For experiments monitoring proton efflux, cells were harvested by exposure to trypsin solution and seeded at a density of 7–10 × 10^4 cells/cm^2 on porous polycarbonate membranes (Transwell, 12-mm diameter, 3-μm pore size; Corning, Inc. Costar, Corning, NY) in α-MEM (catalog no. 12571) supplemented with HCO_3^- (26 mM), FBS (10% vol/vol), and antibiotics (1% vol/vol), pH 7.30 ± 0.02. Cultures were grown in 5% CO_2 at 37 C for 48 h.

For studies of $[Ca^{2+}]_i$, lactate efflux or glucose uptake, cells were seeded (5 × 10^4 cells/cm^2) on 60-mm culture dishes (Becton Dickinson and Co., Lincoln Park, NJ) in supplemented α-MEM for 48–72 h. For experiments examining lactate efflux, growth medium was replaced with α-MEM supplemented with bovine albumin (1 mg/ml) and antibiotic solution (1% vol/vol), on the day of the experiment.

Measurement of proton efflux

Cells adhering to the polycarbonate membranes were placed in microflow chambers and positioned above silicon-based potentiometric sensors, which can detect changes in extracellular pH of as little as 10^{-3} units (Cytosensor microphysiometer, Molecular Devices, Sunnyvale, CA) (14). Cells were continuously superfused at a rate of 100 μl/min with medium at 37 C. Superfusion media with low buffering power were used to enhance the small alterations in pH_o arising because of efflux of protons from cells. Each chamber was supplied with medium from one of two reservoirs by a computer-controlled valve. Test substances were directly introduced in superfusion medium, and changes in proton efflux were monitored. The lag time between a valve switch and the arrival of test solutions at the microflow chambers was 4–5 sec.

Surface potential of each silicon sensor, corresponding to the extracellular pH (pH_o), was plotted as a voltage-time trace. At 37 C, 61 mV corresponds to 1 pH unit. To measure the rate of acidification (net cellular efflux of proton equivalents), fluid flow to cells was stopped periodically for 30 sec. During this time, acid accumulated in the microflow chamber (vol, 2.8 μl) causing pH_o to decrease. Measurement of acidification rate was obtained by linear least-squares fit to the slope of the pH_o-time trace during the time when fluid flow to the cells was stopped. Net cellular efflux of proton equivalents (proton efflux) was calculated from the acidification rate, based on the buffering power of the superfusion solution and volume of the microflow chamber. In experiments examining the role of cytosolic Ca^{2+} in CT-induced proton efflux, cells were loaded with BAPTA-AM (50 μM in conditioned medium) for 30 min at 37 C before placement in microflow chambers. To test for possible nonspecific interactions with silicon sensors, cultures were lysed using detergent solution and then superfused with CT solution or test media.

Measurement of $[Ca^{2+}]_i$

Cells expressing C1a, CTRΔe13, or empty vector, were loaded with indo-1 by incubation in conditioned medium with indo-1 AM (2 μM) for 30 min at 37 C. Cells were then washed and harvested by 1-min exposure to trypsin solution. Conditioned medium was added to inactivate trypsin; and subsequently, cells were sedimented and resuspended in HEPES-buffered MEM (catalog no. 41200). Aliquots of cell suspension were sedimented and resuspended in 2 ml of continuously stirred Na^+-HEPES buffer in a fluorometric cuvette maintained at 37 C. Test substances were added directly to the cuvette.

$[Ca^{2+}]_i$ was monitored using a dual-wavelength fluorimeter (Model RF-M2004, from Photon Technology International, South Brunswick, NJ) at 355 nm excitation and emission wavelengths of 405 and 485 nm. The system software was used to subtract background fluorescence and calculate the ratio, R, which is the fluorescence intensity at 405 nm

divided by the intensity at 485 nm. $[Ca^{2+}]_i$ was determined from the relationship $[Ca^{2+}] = K_d [(R\text{-}R_{min})/(R_{max}\text{-}R)]\beta$, where K_d (for the indo-1-Ca^{2+} complex) was taken as 250 nM, R_{min} and R_{max} were the values of R at low and saturating concentrations of Ca^{2+}, respectively, and β was the ratio of the fluorescence at 485 nm measured at low and saturating Ca^{2+} concentration (15).

Measurement of lactate efflux and glucose uptake

Extracellular lactate was measured using a spectrophotometric assay based on generation of NADH via catalytic action of lactate dehydrogenase (Sigma lactate assay kit, catalog no. 826). Cultures were incubated with CT or vehicle in serum-free α-MEM (catalog no. 12571) containing bovine albumin (1 mg/ml) in 5% CO_2 at 37 C. Samples of media (100 μl) were collected for lactate determination; and, at the end of each experiment, cells were harvested for protein measurement.

Initial rates of glucose uptake by C1a cells were measured using radiolabeled 2-deoxyglucose, as described previously (16). Briefly, cultures were incubated for 1 min at 23 C with 2-deoxy-D-[^{3}H]glucose (60 μM, specific activity adjusted with unlabeled 2-deoxyglucose to 3.3 mCi/mmol) in glucose-free transport buffer. Incubations were terminated by washing with ice-cold isosmotic Tris-sucrose solution and cells were harvested for protein determination and scintillation counting.

Data analysis and statistics

Proton efflux was normalized as a percentage of basal efflux in standard superfusion medium before addition of test substance or change of superfusion solution. This normalization compensated for differences in cell numbers among the chambers. Basal levels of $[Ca^{2+}]_i$ were determined 50 sec before application of test substance. Peak Ca^{2+} responses were quantified as the maximum elevation of $[Ca^{2+}]_i$ above basal levels induced by the test substance. Results are presented as representative traces or as means ± SE of the number of samples indicated. Sigmoid curves were fit by nonlinear regression using Prism (GraphPad Software, Inc., San Diego, CA). Comparisons among means were performed by ANOVA followed by a Tukey-Kramer test for multiple comparisons. Differences were accepted as statistically significant at $P < 0.05$.

Results

Effects of CT on proton efflux

Proton efflux from HEK293 cells, stably transfected with the C1a receptor isoform, CTRΔe13 isoform, or empty vector, was monitored using microphysiometry. Basal proton efflux in standard superfusion medium remained steady for periods of at least 6 h. In C1a cells, superfusion with CT (10 nM) caused a rapid biphasic increase in proton efflux characterized by an initial transient (which reached maximum in 1.5–3 min and lasted approximately 8 min) and a sustained plateau (which lasted for periods of at least 4 h) (Fig. 1A). Treatment with vehicle did not cause any appreciable change in proton efflux. Because the CTRΔe13 isoform binds CT with lower affinity than does the C1a isoform, higher concentrations of CT were used to test CTRΔe13 cells. In contrast to its effect on C1a cells, CT (0.1–1 μM) did not elicit detectable changes in proton efflux from either CTRΔe13 cells (Fig. 1B) or control cells transfected with empty vector (Fig. 1C).

In C1a cells, we investigated the dependence of the increase in proton efflux on CT concentration. Responses to lower concentrations of CT (1–100 pM) consisted of a plateau only. On the other hand, the response to higher concentrations of CT (≥1 nM) included both an initial transient and sustained plateau (Fig. 2A). The initial phase of the CT response was quantified as the maximal increase in proton efflux above basal within 4.5 min of application of CT (Fig. 2B). The plateau was quantified as the average increase in proton efflux above basal, 21–25.5 min after application of CT (Fig. 2C). The concentrations of CT required to elicit an EC_{50} in proton efflux were 10 and 30 pM (for the sustained and initial phases, respectively; Fig. 2, C and B).

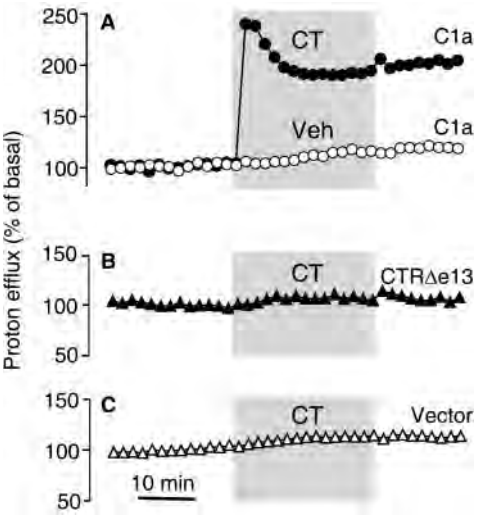

FIG. 1. CT causes a biphasic increase in proton efflux from C1a cells. HEK293 cells transfected with the CTR isoform C1a (A), CTRΔe13 (B), or empty vector (C) were cultured on porous polycarbonate membranes, and proton efflux was monitored by microphysiometry. Cells were superfused with standard medium and, at 1.5-min intervals, superfusion was interrupted for 30 sec to measure acidification rate. Proton efflux (net efflux of proton equivalents) was calculated from the acidification rate and expressed as a percentage of basal proton efflux. Where indicated by the *shaded areas*, C1a cells were superfused with CT (10 nM) or vehicle (Veh), and CTRΔe13 cells and control cells were superfused with CT (100 nM). Results are representative responses from at least three separate cell preparations. Mean values of basal proton efflux per sample were (in nmol proton equivalents/min): C1a cells, 0.19 ± 0.02 (mean ± SE, n = 128); CTRΔe13 cells, 0.10 ± 0.02 (n = 21); Vector, 0.11 ± 0.02 (n = 8).

We then examined the effect of sequential applications of CT on proton efflux from C1a cells. Initial superfusion with a maximally effective concentration of CT (10 nM) caused a biphasic increase in proton efflux (initial phase, 91 ± 16%; sustained plateau, 63 ± 15%; n = 7; Fig. 3). Subsequently, cells were superfused with standard medium for periods of 0.5–2.5 h. A second application of CT (10 nM) did not induce any additional increase in proton efflux, regardless of the time between challenges. These findings are in keeping with the poor reversibility of CT binding to its receptors. On the other hand, initial superfusion with a submaximal concentration of CT (10 pM) increased proton efflux to plateaus of 25 ± 6% above basal (n = 3). Subsequently, cells were superfused with standard medium for 30 min, after which application of CT (10 nM) elevated proton efflux (initial phase, 100 ± 8% and sustained plateau, 76 ± 5% above basal values calculated immediately before superfusion with 10 pM CT; n = 3). The second response was not significantly different from the control response to CT (10 nM) in parallel samples of naive cells (initial phase, 86 ± 10%; sustained plateau, 61 ± 9%; n = 4). Thus, no evidence was found for desensitization.

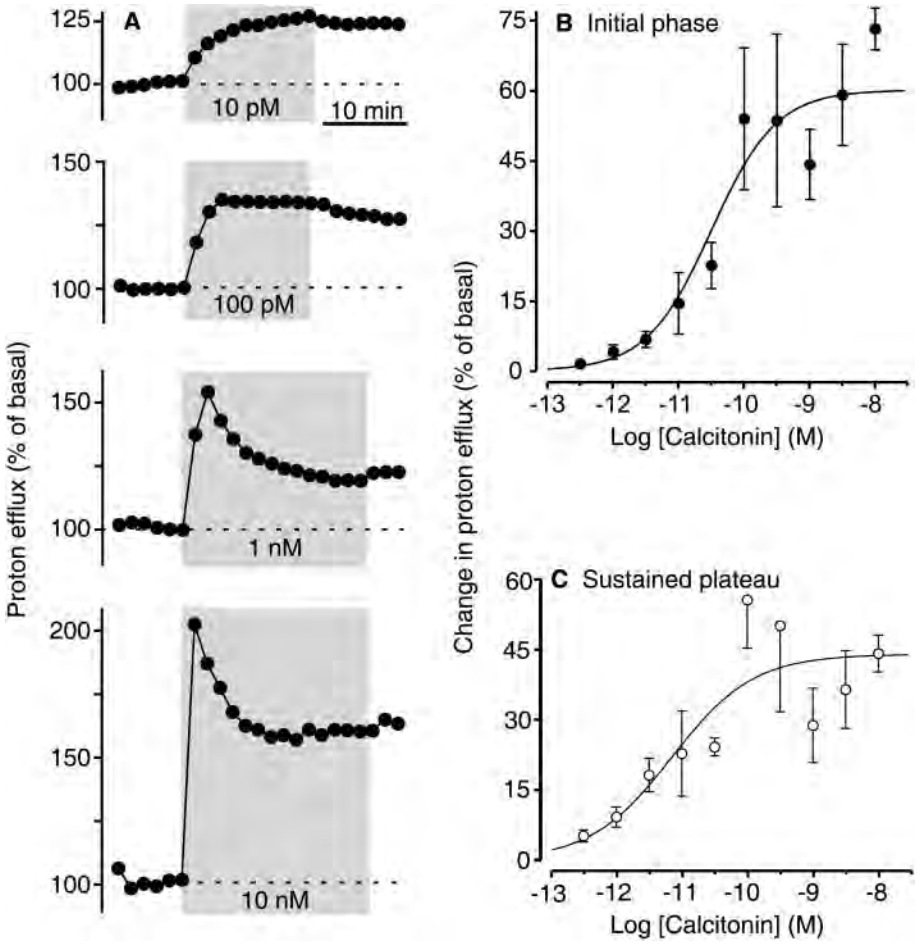

FIG. 2. Increase in proton efflux from C1a cells is dependent on CT concentration. C1a cells were superfused with standard medium, and proton efflux was monitored. A, Representative time courses of changes in proton efflux induced by the indicated concentrations of CT. B and C, Cell samples were superfused with the indicated concentrations of CT in standard medium for 15–21 min. B, Maximum amplitude of the initial phase (above basal) was measured within 4.5 min of application of CT. C, Data are amplitude of the sustained plateau phase, quantified as the average increase in proton efflux above basal, 21–25.5 min after application of CT. Data in B and C are means ± SE from at least four separate cell preparations. EC_{50}s were 30 and 10 pM CT in B and C, respectively. Mean value of basal proton efflux per sample was 0.196 ± 0.002 nmol proton equivalents/min (n = 107).

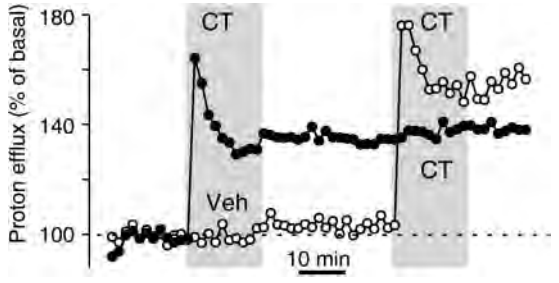

FIG. 3. Effect on proton efflux of sequential treatments with CT. C1a cells were superfused with standard medium, and proton efflux was monitored by microphysiometry. Where indicated by the *shaded areas*, cells were superfused with CT (10 nM) or vehicle (Veh) in standard medium. Results are from parallel samples and are representative of responses from four separate cell preparations. Values of basal proton efflux per sample were (in nmol proton equivalents/min): CT, 0.07; Veh, 0.12.

Role of Na^+/H^+ exchange in CT-induced proton efflux

Next, we investigated the mechanisms underlying the effects of CT on proton efflux from C1a cells. Na^+/H^+ exchange is an important pathway for proton efflux and plays a role in the regulation of cytosolic pH, maintenance of cell volume, and transcellular Na^+ transport. To assess the involvement of Na^+/H^+ exchange, we first used amiloride, an inhibitor of the Na^+/H^+ exchanger isoforms NHE-1, 2, and 5 (17, 18).

C1a cells were treated with amiloride (500 μM) or vehicle in standard superfusion medium. Treatment with amiloride caused a slight decrease in proton efflux (to ~95% of basal levels). Subsequently, cells were treated with CT (10 nM) in the continued presence of amiloride or vehicle. Amiloride abolished the transient component of the initial phase of the CT response (Fig. 4A). Cells were then superfused with either amiloride or vehicle, before returning to standard superfusion medium. A rapid overshoot in proton efflux was observed upon washout of amiloride. Subtracting the response to CT in the presence of amiloride from the control response revealed the amiloride-sensitive component (Fig. 4Aii). This component accounts for the transient portion of the initial phase of the CT response. Consistent with the pattern observed in Fig. 4Aii, an increase in the set point of the Na^+/H^+ exchanger, to a more alkaline value of cytosolic pH, causes a transient increase in proton efflux by the exchanger, lasting only until a new alkaline steady-state value is reached.

Because amiloride inhibits several isoforms of the Na^+/H^+ exchanger, we next used cariporide (HOE 642), a potent and highly selective inhibitor of NHE-1 (19). Like amiloride, cariporide (5 μM) abolished the initial transient but not the sustained plateau (Fig. 4B). The cariporide-sensitive component of the CT response was virtually identical to the amiloride-sensitive efflux (Fig. 4Bii). Taken together, these data establish that the initial transient portion

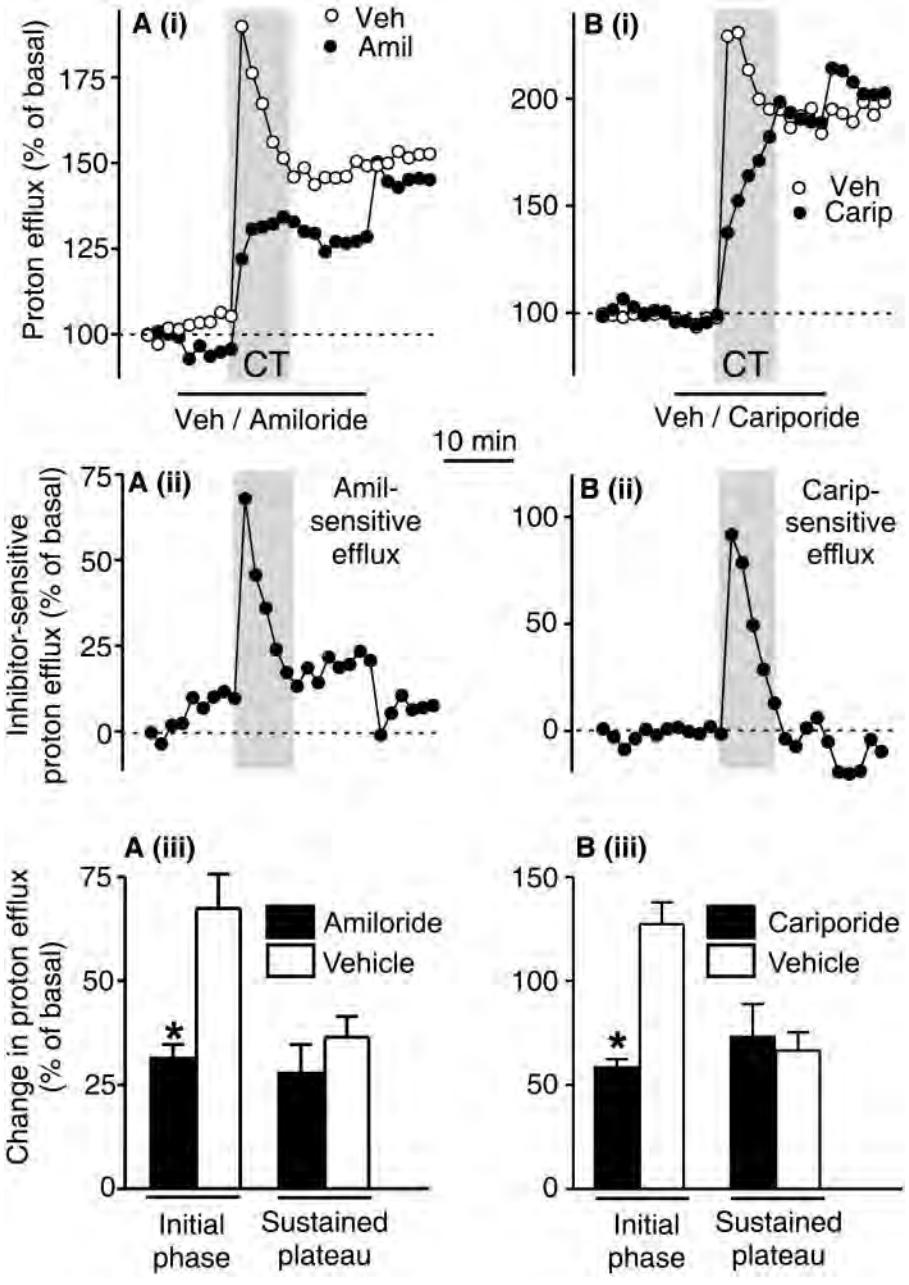

FIG. 4. The initial transient component of the CT-induced increase in proton efflux is inhibited by NHE blockers. C1a cells were superfused with standard medium, and proton efflux was monitored. A (i), Parallel samples were exposed to vehicle (Veh) or amiloride (Amil, 500 μM) for the period indicated by the *horizontal bar beneath the graph*. After equilibration for 7.5 min, cultures were superfused with CT (10 nM) where indicated by the *shaded area*, in the continued presence of Veh or amiloride. A (ii), The amiloride-sensitive component of the CT response, obtained by subtracting the proton efflux in the presence of amiloride from the proton efflux in the presence of Veh. A (iii), *Bars* represent amplitudes of initial phase and sustained plateau induced by CT in the presence of Veh or amiloride. Data are changes in proton efflux above basal expressed as percentage of basal efflux (means ± SE of four samples from three separate cell preparations; *, $P < 0.05$ for the effect of amiloride). Mean values of basal proton efflux per sample were (in nmol proton equivalents/min): 0.12 ± 0.02 for Veh and 0.20 ± 0.05 for amiloride. B, The same protocol described in A was used to investigate the effects of cariporide (Carip, 5 μM, a selective blocker of NHE-1) on the increase in proton efflux induced by CT (10 nM). Data in B (iii) are means ± SE of three samples from two separate cell preparations, * $P < 0.05$ for the effect of Carip. Mean values of basal proton efflux per sample were (in nmol proton equivalents/min): 0.07 ± 0.02 for Veh and 0.09 ± 0.03 for Carip.

of the CT-stimulated increase in proton efflux from C1a cells is attributable to NHE-1 activity.

It has been previously shown that CT stimulates H^+ secretion from rat kidney intercalated cells via a bafilomycin A_1-sensitive mechanism (20), likely the vacuolar H^+-ATPase. We used the specific inhibitor, bafilomycin A_1, to examine the possible involvement of the vacuolar H^+-ATPase in CT-induced proton efflux. C1a cells were treated with bafilomycin (100–500 nM) or vehicle in standard superfusion medium. Treatment with bafilomycin did not affect basal proton efflux. Proton efflux induced by 10 nM CT in the presence of bafilomycin A_1 (initial phase, 79 ± 11%; sustained plateau, 38 ± 3%; n = 7) was not significantly different from responses in the presence of vehicle (initial phase, 65 ± 5%; sustained plateau, 31 ± 4%; n = 8), arguing against a role for the vacuolar H^+-ATPase.

Dependence of CT-induced proton efflux on extracellular glucose

We next considered the possibility that the sustained plateau phase of the CT-induced increase in proton efflux is caused by enhanced metabolism of glucose. Parallel samples of C1a cells were superfused with standard medium (containing 5 mM glucose) or glucose-free medium. Superfusion with glucose-free medium rapidly decreased basal proton efflux to 43 ± 5% of control levels (Fig. 5Ai, mean ± SE, n = 8), indicating that basal efflux is highly sensitive to changes in the availability of glucose. Cells were then exposed to CT

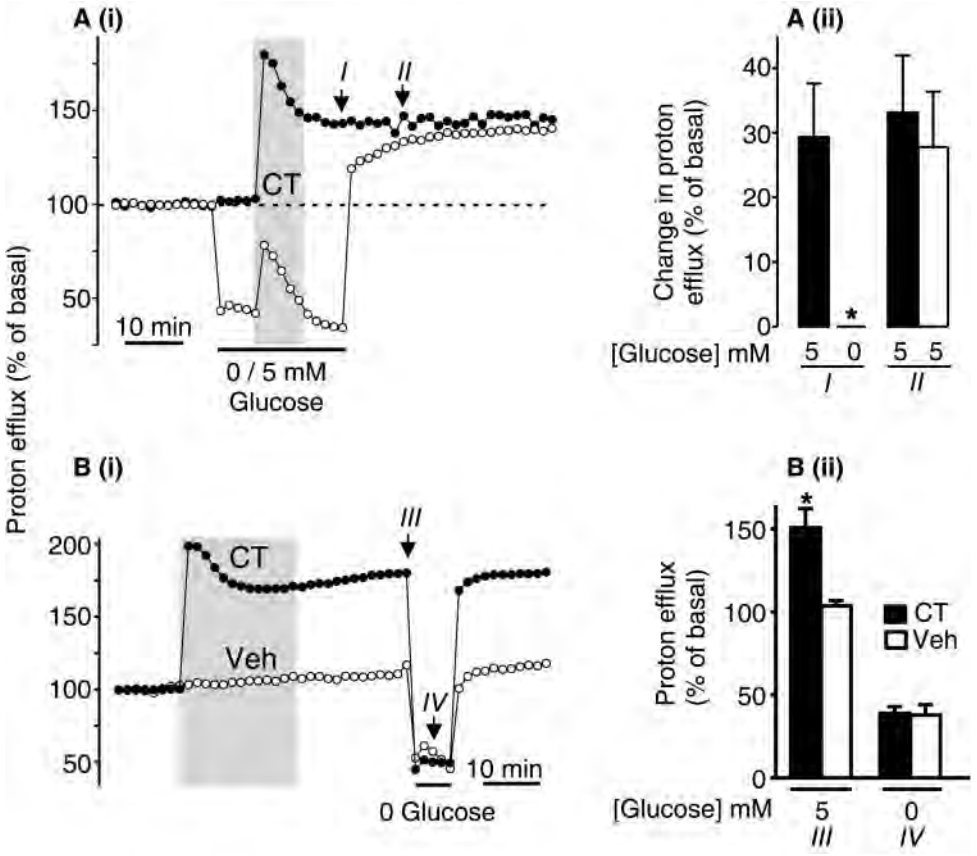

FIG. 5. Dependence of the CT-induced increase in proton efflux on extracellular glucose. Proton efflux from C1a cells was monitored using microphysiometry. A (i), Parallel samples were initially superfused with standard medium. Subsequently, samples were superfused with either glucose-free medium (0 glucose, *open circles*) or standard medium (5 mM glucose, *closed circles*) for the period indicated by the *horizontal bar beneath the graph*. After equilibration for 7.5 min, cultures were superfused with CT (10 nM) where indicated by the *shaded area*, in the continued presence of appropriate media. A (ii), Amplitude of the plateau calculated at the times indicated by *I* and *II* in A (i). The *filled bar* represents the response of cells in the continuous presence of 5 mM glucose. The *unfilled bar* represents the response of cells exposed to glucose-free medium. The amplitude of the plateau at *I* was calculated as the change in proton efflux from the level immediately before superfusion with CT. The amplitude of the plateau after return to standard (glucose-containing) superfusion medium (*II*) was calculated as the change in proton efflux from the level immediately before the initial change in superfusion medium. Amplitudes are expressed as percentage of basal proton efflux and are means ± SE of 8–10 samples from at least 6 separate cell preparations; *, $P < 0.05$ for the effect of glucose removal. Mean values of basal proton efflux per sample were (in nmol proton equivalents/min): 0.15 ± 0.03 for 5 mM glucose and 0.17 ± 0.04 for glucose-free. B (i), Parallel samples of C1a cells were superfused with standard medium. Cells were then treated with CT (10 nM) or vehicle (Veh) where indicated by the *shaded area*. Subsequently, both samples were superfused with glucose-free medium where indicated by the *horizontal bar*. B (ii), Values of proton efflux calculated at the times indicated by *III* and *IV* in B (i). Data are expressed as percentage of basal proton efflux (calculated immediately before superfusion with CT or Veh) and are means ± SE of 6–7 samples from 5 separate cell preparations; *, $P < 0.05$ for the effect of CT. Mean values of basal proton efflux per sample were (in nmol proton equivalents/min): 0.40 ± 0.07 for CT and 0.30 ± 0.10 for Veh.

(10 nM) in the presence or absence of glucose. We observed that the removal of glucose virtually abolished the sustained plateau phase of the CT response, leaving the initial transient component intact. Upon reintroduction of glucose, proton efflux recovered to levels comparable with the sustained plateau in control cells exposed to CT in the presence of glucose (Fig. 5Aii).

To confirm the role of extracellular glucose in the plateau phase of the CT response, parallel samples were treated with CT (1–30 nM) or vehicle. Subsequently, when both CT- and vehicle-treated cells were superfused with glucose-free medium (7.5–20 min), there was a large rapid decrease in proton efflux, to comparable levels (Fig. 5Bii). Thus, the plateau phase is completely dependent on extracellular glucose, suggesting that glucose metabolism underlies this phase of the response to CT.

Based on its dependence on extracellular glucose, it is possible that lactic acid production plays a role in the sustained plateau phase of proton efflux. To investigate the effect of CT on lactic acid efflux, C1a cells were incubated with either CT (10 nM) or vehicle, and CTRΔe13 cells were incubated with CT (1 μM) or vehicle for 2 h. CT caused a significant increase in lactate efflux from C1a cells but had no significant effect on lactate efflux from CTRΔe13 cells (Fig. 6). The amplitude of the CT-induced increase in lactate efflux (~50%) in C1a cells was comparable with that of the sustained increase in proton efflux (~44%) induced by CT. Thus, the plateau phase of the CT-induced increase in proton efflux seems to arise by enhanced glycolysis. We next examined whether this effect involved enhanced glucose transport. CT had no significant effect on the initial rate of 2-deoxyglucose uptake (380 ± 63 nmol [^{3}H]deoxyglucose/g cell protein·min

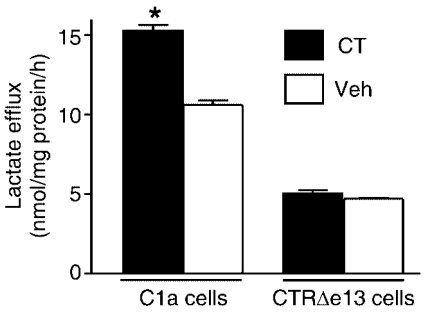

FIG. 6. Effect of CT on lactate production. C1a and CTRΔe13 cells were treated with CT (10 nM or 1 μM, respectively) or vehicle (Veh) in α-MEM containing bovine albumin (1 mg/ml) for 2 h. Samples of extracellular medium were collected for lactate determination, and cells were harvested for protein determination. Lactate efflux is expressed as nmol lactate/(μg cell protein·h). Values are means ± SE of at least three samples from two separate experiments; *, $P < 0.05$ for the effect of CT.

in control cells; 358 ± 69 nmol [^{3}H]deoxyglucose/g cell protein·min in cells pretreated with 10 nM CT for 15 min, mean ± SE, n = 6 separate experiments). These findings indicate that CT-induced proton efflux does not arise simply from an increase in the rate of glucose uptake.

Role of cAMP in CT-induced increase in proton efflux

The EC_{50} reported in our studies for the effect of CT on proton efflux is similar to the value reported previously for CT-mediated increases of cAMP levels in C1a cells (10). However, although CT leads to elevation of cAMP in both C1a and CTRΔe13 cells, it failed to induce an increase in proton efflux from CTRΔe13 cells, arguing against a role for this second messenger in mediating CT-induced proton efflux from C1a cells.

To further investigate the involvement of cAMP in regulating proton efflux, we examined the effects of CPT-cAMP (a membrane-permeable, phosphodiesterase-resistant analog of cAMP). Maximally effective concentrations of CPT-cAMP (0.1–1 mM) induced only a small increase in proton efflux from C1a cells, to 7 ± 1% above basal (n = 21). Moreover, CPT-cAMP had no significant effect on the subsequent response of C1a cells to CT (10 nM) (Table 1). Next, we examined the effects of the phosphodiesterase inhibitor, IBMX. IBMX (40 μM) induced a small increase in proton efflux but did not potentiate the subsequent response of C1a cells to CT (1–10 nM) (Table 1). Even at higher concentrations, IBMX did not potentiate the response to CT. In C1a cells treated with IBMX (0.1–1 mM), the increase in proton efflux induced by 1 nM CT (initial phase, 84 ± 9%; sustained plateau, 58 ± 6%; n = 7) was not significantly different from the response to CT in vehicle-treated control cells (initial phase, 81 ± 13%; sustained plateau, 56 ± 7%; n = 6). Taken together, these data suggest that elevation of cAMP does not underlie the CT-induced increase in proton efflux from C1a cells.

Effect of CT on the $[Ca^{2+}]_i$

To further characterize the signaling pathways underlying the actions of CT on proton efflux from C1a cells, we next

TABLE 1. Role of cAMP in regulating proton efflux from C1a cells

Treatment	Change in proton efflux (% basal)			n
	Effect of treatment alone	CT-induced initial transient	CT-induced sustained plateau	
Vehicle	0 ± 0	65 ± 12	48 ± 10	6
CPT-cAMP	2 ± 3	47 ± 1	25 ± 8	3
IBMX	14 ± 2	72 ± 12	42 ± 5	4

C1a cells were superfused with standard medium, and proton efflux was monitored using microphysiometry. Parallel samples were treated with vehicle, the cAMP analog (CPT-cAMP, 0.1–0.5 mM), or the phosphodiesterase inhibitor (IBMX, 40 μM) for 10.5–15 min. Samples were then treated with CT (1–10 nM) in the continued presence of either vehicle, CPT-cAMP, or IBMX for 10.5–15 min. Data are changes in proton efflux expressed as percentage of basal values determined immediately before the initial treatment. Data are means ± SE for n samples from at least two separate cell preparations. There were no significant differences between vehicle-treated samples and those treated with CPT-cAMP or IBMX. Mean values of basal proton efflux per sample were (in nmol proton equivalents/min): 0.30 ± 0.03 for CPT-cAMP and IBMX, and 0.20 ± 0.07 for vehicle.

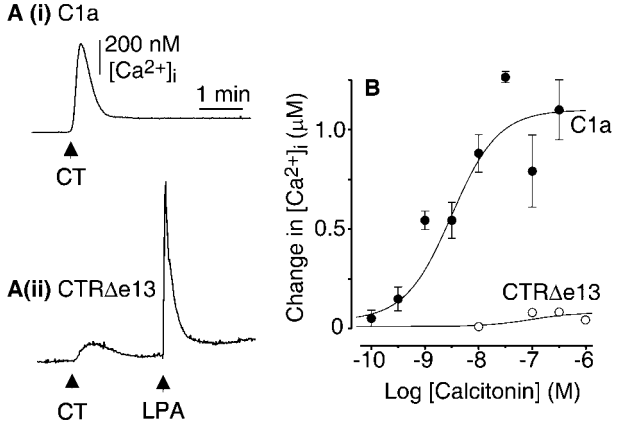

FIG. 7. Effect of CT and LPA on $[Ca^{2+}]_i$. C1a and CTRΔe13 were loaded with Ca^{2+}-sensitive dye indo-1 and suspended in Ca^{2+}-containing Na^+-HEPES buffer in a fluorometric cuvette at 37 C with continuous stirring. $[Ca^{2+}]_i$ was monitored by fluorescence spectrophotometry. A, Where indicated by the *arrows*, CT (1 nM for C1a cells or 100 nM for CTRΔe13 cells) or LPA (10 μM) was added directly to the cuvette. Traces are representative of the responses of at least 3 separate cell preparations. B, Single applications of CT were made to individual samples of C1a or CTRΔe13 cells at the concentrations indicated. Data are amplitude of maximal elevations of $[Ca^{2+}]_i$ above resting levels and are means ± SE of 3–14 samples for each point, from ≥ 2 separate cell preparations. *Error bars* for CTRΔe13 data were smaller than the symbols.

investigated the effect of CT on $[Ca^{2+}]_i$. C1a cells, CTRΔe13 cells, and cells transfected with empty vector were loaded with the Ca^{2+}-sensitive dye indo-1, and changes in $[Ca^{2+}]_i$ were monitored using fluorescence spectrophotometry. In C1a cells, CT (1 nM) rapidly induced a large transient elevation of $[Ca^{2+}]_i$, to peaks 544 ± 47 nM above basal levels of 163 ± 15 nM (mean ± SE, n = 23, Fig. 7Ai). In contrast, even at CT concentrations of up to 1 μM, there was either no Ca^{2+} response or only a small elevation of $[Ca^{2+}]_i$ in control cells (transfected with empty

vector) and in CTRΔe13 cells (Fig. 7Aii).[1] These findings indicate that CT-induced changes in $[Ca^{2+}]_i$ are mediated selectively by the C1a receptor.

To confirm the responsiveness of CTRΔe13 cells, we also examined effects of LPA, which acts through G protein-coupled receptors to evoke elevation of $[Ca^{2+}]_i$ in a number of target tissues (21). In CTRΔe13 cells previously exposed to CT, LPA (10 μM) induced rapid elevation in $[Ca^{2+}]_i$, to 656 ± 74 nM above basal levels of 126 ± 12 nM (Fig. 7Aii, n = 18). This finding establishes the presence of abundant intracellular Ca^{2+} stores and cellular machinery supporting receptor-induced elevation of $[Ca^{2+}]_i$ and argues against the existence of a signal from the CTRΔe13 receptor that inhibits Ca^{2+} mobilization.

Next, we examined the dependence of the amplitude of the Ca^{2+} response on CT concentration (Fig. 7B). The EC_{50} for the effects of CT on elevation of $[Ca^{2+}]_i$ in C1a cells was 1–3 nM, similar to that reported for CT-induced production of inositol phosphates in C1a cells (10) but 100-fold greater than the EC_{50} obtained for effects of CT on proton efflux (compare Figs. 2, B and C, with 7B).

We then investigated whether activation of phospholipase C played a role in the CT-induced elevation of $[Ca^{2+}]_i$ in C1a cells. Cells were pretreated with U-73122, a PLC inhibitor, or U-73343, an inactive analog (3 μM, 10.5 min), and were resuspended in Na^+-HEPES buffer containing inhibitor or inactive analog. U-73122 virtually abolished the Ca^{2+} response to CT, implicating PLC in this response. In contrast, after pretreatment with U-73343, CT (1 nM) induced an elevation in $[Ca^{2+}]_i$ similar to responses observed in untreated C1a cells (Table 2).

TABLE 2. Effects of phospholipase C inhibition on elevations of $[Ca^{2+}]_i$ in C1a cells

Treatment	Basal $[Ca^{2+}]_i$ (nM)	CT-induced change in $[Ca^{2+}]_i$ (nM)	*n*
Untreated	163 ± 15	544 ± 47	23
U-73122	268 ± 38[a]	18 ± 8[a]	10
U-73343	124 ± 12	670 ± 104	6

C1a cells were loaded with Ca^{2+}-sensitive dye indo-1. Cells were pretreated with U-73122 (3 μM), an inhibitor of PLC, or its inactive analog U-73343 (3 μM) for 10.5 min. Cells were then suspended in Na^+-HEPES buffer alone or in buffer containing U-73122 or U-73343. Changes in $[Ca^{2+}]_i$ were monitored by fluorimetry. CT (1 nM) was added directly to the cuvette. Values are basal levels of $[Ca^{2+}]_i$ and CT-induced maximal elevations of $[Ca^{2+}]_i$ above basal levels and are means ± SE for *n* cell samples from at least three separate cell preparations.

[a] $P < 0.05$, compared with untreated control.

Elevation of cytosolic Ca^{2+} suppresses proton efflux

C1a cells, but not CTRΔe13 cells, respond to CT with large elevations in $[Ca^{2+}]_i$, reflecting the selective effects of CT on proton efflux from C1a but not CTRΔe13 cells. To test whether elevations in $[Ca^{2+}]_i$ mediate an increase in proton efflux, we used the Ca^{2+} ionophore, ionomycin, and the sarco-endoplasmic reticulum Ca^{2+}-ATPase (SERCA) inhibitor, thapsigargin. Ionomycin (100 nM) and thapsigargin (1 μM) elevated $[Ca^{2+}]_i$ to 538 ± 63 (mean ± SE, n = 6) and 334 ± 75 nM (n = 7) above basal levels of 130 ± 22 and 114 ± 27 nM, respectively (Fig. 8A), comparable with CT-induced elevations of $[Ca^{2+}]_i$ in C1a cells of 544 ± 47 nM above basal levels of 163 ± 15 nM.

Proton efflux from parallel samples of C1a cells was then monitored. Superfusion of cells with ionomycin (1 μM)[2] or thapsigargin (1 μM) induced a gradual decrease in proton efflux, to 26 ± 2% and 37 ± 21% below basal, respectively (n = 3). Proton efflux returned slowly to basal levels after washout of ionomycin but not thapsigargin (Fig. 8B). Our observation that ionomycin and thapsigargin suppressed, rather than enhanced, proton efflux suggests that elevation of $[Ca^{2+}]_i$ alone does not lead to the increase in proton efflux induced by CT.

To further assess the role of CT-induced elevation of $[Ca^{2+}]_i$ in proton efflux, we loaded cells with the intracellular Ca^{2+} chelator, BAPTA. We have previously reported that loading C1a cells using BAPTA-AM (50 μM, 30 min) reduced the amplitude of the elevation of $[Ca^{2+}]_i$ induced by CT (1 nM), from 319 ± 37 nM to 53 ± 4 nM above basal (13). In the present study, C1a cells were loaded with BAPTA under the same conditions, and proton efflux in response to CT was monitored. CT-induced increases in proton efflux were still observed in BAPTA-loaded cells, indicating that a large elevation of $[Ca^{2+}]_i$ is not necessary for this response (data not shown).

Effect of PKC activation on proton and lactate efflux

In a number of tissues, PKC plays a role in agonist-mediated activation of Na^+/H^+ exchange and glycolysis (22–24). Therefore, we investigated the possible role of PKC in mediating the CT-induced increase in proton and lactate efflux.

TPA is a potent activator of the conventional and novel PKC isoforms. In parallel samples of C1a cells, TPA (100 nM) caused a sustained increase in proton efflux, mimicking the plateau phase of the response to CT (Fig. 9A). When vehicle-treated control cells were subsequently treated with CT (10 nM), they responded with a biphasic elevation in proton efflux. However, in cells treated acutely with TPA, CT elicited the initial transient increase in proton efflux but no further increase in the sustained plateau phase. When both samples were treated again with TPA (100 nM), no additional increases in proton efflux were observed.

As a next step, we characterized the TPA-induced increase in proton efflux from C1a cells. When TPA- and vehicle-treated cells were superfused with glucose-free medium, there was a rapid decrease in proton efflux, to comparable levels (Fig. 9B). This finding indicates that, similar to the sustained plateau phase of the CT response, the sustained

[1] The small elevation of $[Ca^{2+}]_i$ in control (vector-transfected) and CTRΔe13 cells was not seen in all experiments. In control cells that did respond, CT (100 nM) induced elevation of $[Ca^{2+}]_i$ to 43 ± 8 nM above basal levels of 97 ± 8 nM (n = 3). Similarly, in responsive CTRΔe13 cells, CT (0.1–1 μM) induced elevation of $[Ca^{2+}]_i$ to 60 ± 7 nM above basal levels of 120 ± 10 nM (n = 22), not significantly different from the response in control cells.

[2] A higher concentration of ionomycin was employed for the proton efflux experiments, because the standard medium contained bovine albumin (1 mg/ml), which bound ionomycin, reducing its apparent potency.

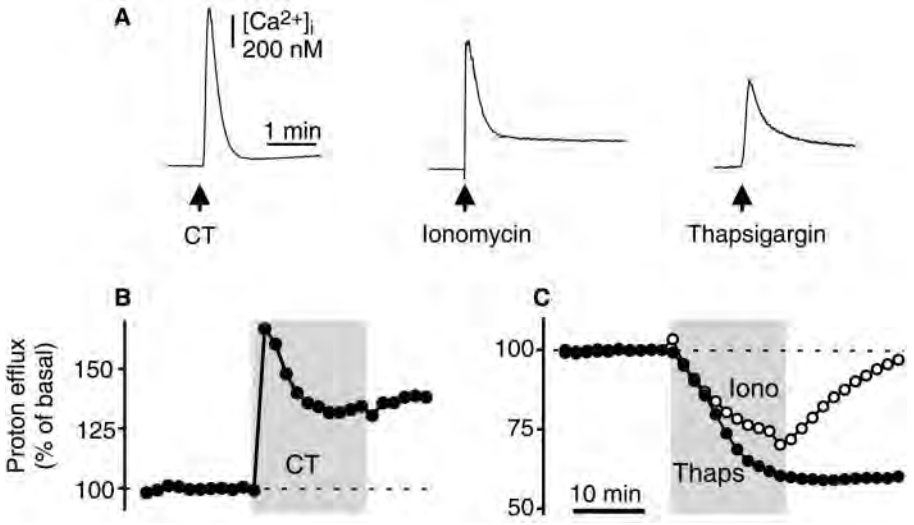

FIG. 8. Elevation of $[Ca^{2+}]_i$ does not increase proton efflux. A, Samples of indo-1-loaded C1a cells were suspended in Na^+-HEPES buffer, and $[Ca^{2+}]_i$ was monitored by fluorimetry. Where indicated by *arrows*, CT (10 nM), the calcium ionophore, ionomycin (100 nM), or the SERCA inhibitor, thapsigargin (1 μM), were directly added to the cuvette. Data are representative of responses from at least three separate cell preparations. B and C, Proton efflux from C1a cells was monitored using microphysiometry. Where indicated by the *shaded area,* cells were treated with CT (10 nM), ionomycin (Iono, 1 μM) or thapsigargin (Thaps, 1 μM) in standard medium. Traces are representative of responses of $\geq$ three samples from at least two separate cell preparations. Mean values of basal proton efflux per sample in standard medium were (in nmol proton equivalents/min): 0.52 $\pm$ 0.09 (n = 3) for ionomycin-treated cells and 0.5 $\pm$ 0.3 for thapsigargin-treated cells.

increase in proton efflux induced by TPA is entirely dependent on extracellular glucose (compare Figs. 5B and 9B).

Because CT failed to elicit an increase in proton or lactate efflux from CTRΔe13 cells, we investigated the responsiveness of these cells to TPA. First, parallel samples of CTRΔe13 cells were treated with CT (1 μM) or vehicle. In both cases, subsequent application of TPA (100 nM) caused a sustained increase in proton efflux similar to that seen in C1a cells (after CT, 41 $\pm$ 2% above basal, n = 10; following vehicle, 61 $\pm$ 11% above basal, n = 2; Fig. 10A). These data rule out the possibility that CT activates a signaling mechanism that inhibits PKC-induced proton efflux. We next examined the effects of TPA on lactate efflux from C1a and CTRΔe13 cells. TPA (100 nM) stimulated lactate efflux from both C1a and CTRΔe13 cells (Fig. 10B). As shown in Fig. 6, basal lactate efflux from CTRΔe13 cells was considerably lower than that from C1a cells; however, the absolute effect of TPA on lactate efflux was almost as much in CTRΔe13 cells as in C1a cells, indicating that the CTRΔe13 cells are capable of increasing glycolysis in response to activation of PKC.

Taken together, these findings suggest the involvement of PKC in mediating the plateau phase of the CT-induced increase in proton efflux.

Effect of PKC inhibition or depletion on CT-induced increase in proton efflux

To further assess the role of PKC in the CT-induced increase in proton efflux, we first investigated the effect of the kinase inhibitor staurosporine. On its own, staurosporine (100 nM) did not affect basal proton efflux. However, staurosporine partially inhibited both the initial transient and the sustained plateau phase of the increase in proton efflux induced by CT (10 nM, Fig. 11A). To confirm the effectiveness of staurosporine, we examined its effect on responses to TPA. In vehicle-treated C1a cells, TPA increased proton efflux to plateaus of 27 $\pm$ 5% above basal (mean $\pm$ SE, n = 4). On the other hand, pretreatment with staurosporine (100 nM, 15 min) completely abolished the response to TPA, confirming its effectiveness (data not shown).

We next investigated the effect of bisindolylmaleimide I, a potent and more selective inhibitor of PKC (Fig. 11B). Bisindolylmaleimide I (100 nM) reduced the CT-induced proton efflux by a relatively uniform amount at all times, consistent with partial inhibition of the sustained plateau phase. We also examined the effect of bisindolylmaleimide I on TPA-induced increase in proton efflux. Similar to staurosporine, bisindolylmaleimide I inhibited the effects of TPA on proton efflux (data not shown).

Last, PKC was depleted by chronic treatment with TPA (100 nM for at least 16 h). Depletion of PKC reduced the sustained plateau of the response to CT (10 nM) by approximately 75%, though having little or no effect on the initial transient (Fig. 12). As expected, depletion of PKC virtually abolished subsequent responses to TPA. Taken together, these findings indicate a role for PKC in mediating the sustained plateau phase of CT response in C1a cells.

Discussion

Activation of the C1a CTR isoform increases proton efflux

CT caused a rapid increase in proton efflux from HEK293 cells stably transfected with the C1a CTR isoform but not the CTRΔe13 isoform. This response consisted of an initial transient, usually maximal within 3 min, and a sustained plateau lasting for periods of at least 4 h. Such responses after activation of a G protein-coupled receptor have not been reported previously. The magnitude of the increase in proton efflux was dependent on the concentration of CT. Although the sustained plateau was observed in response to both low

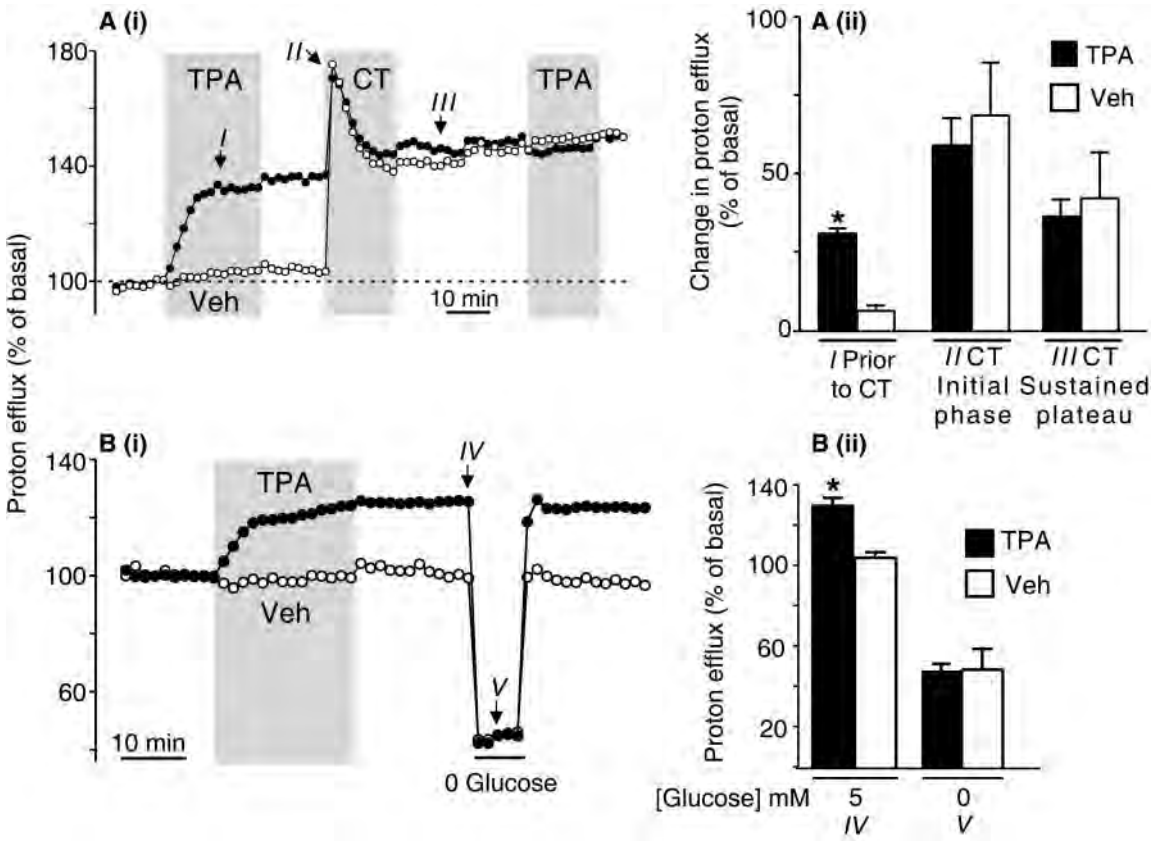

FIG. 9. Effect of a PKC activator on proton efflux from C1a cells. C1a cells were superfused with standard medium, and proton efflux was monitored using microphysiometry. A (i), Parallel samples were treated acutely with the PKC activator, TPA (100 nM), or vehicle (Veh) where indicated by the *first shaded area*. Subsequently, both samples were treated with CT (10 nM) where indicated by the *second shaded area*. Both samples were then treated with TPA (100 nM) where indicated by the *third shaded area*. A (ii), Changes in proton efflux above basal were quantified at the times indicated by *Roman numerals* in A (i) and are expressed as percentage of basal values calculated immediately before superfusion with TPA or Veh. Data are means ± SE of three to five samples from three separate cell preparations; *, $P < 0.05$ for the effect of TPA. Mean values of basal proton efflux per sample were (in nmol proton equivalents/min) 0.08 ± 0.03 for Veh (n = 3) and 0.10 ± 0.02 for TPA (n = 5). B (i), Parallel samples of C1a cells were superfused with standard medium. Cells were then treated with TPA (100 nM) or Veh where indicated by the *shaded area*. Subsequently, both samples were superfused with glucose-free medium where indicated by the *horizontal bar*. B (ii), Values of proton efflux calculated at the times indicated by *IV* and *V* in B (i). Data are expressed as percentage of basal proton efflux (calculated immediately before superfusion with TPA or Veh) and are means ± SE of three to four samples from two separate cell preparations; *, $P < 0.05$ for the effect of TPA. Mean values of basal proton efflux per sample were (in nmol proton equivalents/min): 0.28 ± 0.09 for TPA and 0.30 ± 0.10 for Veh.

and high concentrations of CT, the transient component of the initial phase was observed clearly only at higher concentrations (≥1 nM).

The plateau phase of the response remained sustained in the continued presence of CT and after wash out. After treatment with a maximal concentration of CT, no additional increase in proton efflux was observed in response to a subsequent treatment. A similar sustained response and refractoriness to subsequent challenge has been described for the activation of adenylyl cyclase by the CTR in T47D cells (25). The sustained response in both cases is probably attributable to the nearly irreversible binding of CT to its receptor at physiological pH (3). Prolonged activation of signaling pathways downstream from the C1a isoform may also contribute to the sustained elevation of proton efflux. Internalization of the CTR (26) prevents responses to subsequent treatments with CT, and it is also possible that the internalized receptor continues to transduce signals, in turn maintaining the sustained increase in proton efflux.

Mechanisms underlying the effects of CT on proton efflux

Blockers of Na^+/H^+ exchange (amiloride and cariporide) had negligible effects on basal proton efflux, indicating little activity of the exchanger under resting conditions. In contrast, both the inhibitors abolished the initial transient component of the CT-induced proton efflux. CT seems to rapidly stimulate the exchanger, giving rise to a transient increase in proton efflux that lasts only until a more alkaline steady-state cytosolic pH is established. Use of the Cytosensor microphysiometer allowed us to resolve stimulation of Na^+/H^+ exchange more rapidly than could be accomplished using conventional approaches. On washout of amiloride or cariporide from CT-treated samples, a transient overshoot in proton efflux occurred, consistent with the recovery of Na^+/H^+ exchange activity. At the concentrations used in our studies, cariporide selectively blocks the NHE-1 isoform (19), which is endogenously expressed in HEK293 cells. Taken together, these findings are consistent with NHE-1 mediating

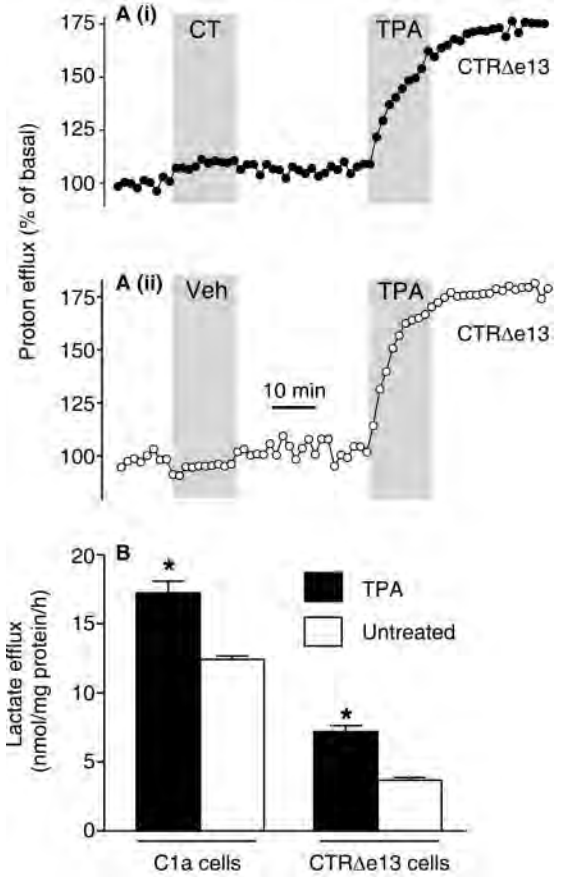

FIG. 10. Effect of a PKC activator on proton and lactate efflux. A, CTRΔe13 cells were superfused with standard medium, and proton efflux was monitored using microphysiometry. Parallel samples were treated with CT [1 μM, A (i)]; or vehicle (Veh) A (ii) followed by the PKC activator, TPA (100 nM) where indicated by the *shaded areas*. Values of basal proton efflux per sample were 0.02 nmol/min for CT-treated and 0.05 for Veh-treated cells. Traces are representative of responses of 10 samples from 3 separate preparations for A (i) and 2 samples from 1 preparation for A (ii). B, C1a and CTRΔe13 cells were incubated with or without TPA (100 nM) in α-MEM containing bovine albumin (1 mg/ml) for 2 h. Samples of extracellular medium were collected for lactate determination, and cells were harvested for protein determination. Lactate efflux is expressed as nmol lactate/(μg cell protein·h). Values are means ± SE of at least 6 samples from 2–3 separate experiments; *, $P < 0.05$ for the effect of TPA.

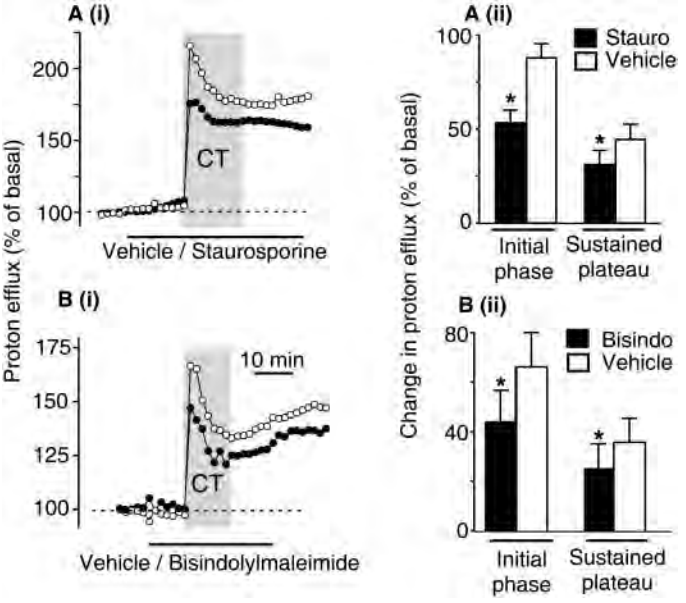

FIG. 11. Effect of protein kinase inhibitors on CT-induced increase in proton efflux. C1a cells were superfused with standard medium, and proton efflux was monitored. A (i), Parallel samples were exposed to Veh or staurosporine (100 nM) for the period indicated by the *horizontal bar beneath the graph*. After equilibration, cultures were superfused with CT (10 nM) where indicated by the *shaded area*, in the continued presence of vehicle (Veh) or staurosporine. A (ii), *Bars* represent amplitudes of initial transients and sustained plateaus induced by CT in the presence of Veh or staurosporine (Stauro). Data are expressed as percentage of basal values and are means ± SE of 12 samples from 5 separate cell preparations; *, $P < 0.05$ for the effect of staurosporine. Mean values of basal proton efflux per sample were (in nmol proton equivalents/min): 0.21 ± 0.03 for Veh and 0.23 ± 0.03 for staurosporine (n = 12). B, The same protocol as described in A above was used to investigate the effects of bisindolylmaleimide I (Bisindo, 100 nM) on the increase in proton efflux induced by CT (10 nM). B (ii), Means ± SE of 7 samples from 4 separate cell preparations; *, $P < 0.05$ for the effect of Bisindo. Mean values of basal proton efflux per sample were (in nmol proton equivalents/min): 0.10 ± 0.02 for Veh and 0.09 ± 0.02 for Bisindo.

the initial transient component of the CT response. In the rabbit renal distal convoluted tubule, CT activates a latent HCO_3^--dependent mechanism, to induce recovery of cytosolic pH after an acid load (27). Under the conditions used in our studies, it is unlikely that HCO_3^- influx contributed to efflux of proton equivalents, because all the superfusion solutions used in the microphysiometer must be nominally HCO_3^- -free to avoid the production of gas bubbles.

In HEK293 cells, basal proton efflux drops to approximately 50% on removal of extracellular glucose. In C1a cells, the sustained plateau, but not the initial transient, is dependent on extracellular glucose. On reintroduction of glucose, proton efflux recovers rapidly to levels comparable with those in control cells treated with CT in the presence of glucose. This indicates that signaling pathways downstream from the CTR have been activated in the absence of glucose, but the sustained plateau is manifested only upon reintroduction of extracellular glucose. Interestingly, CT increased both lactate efflux and proton efflux (during the sustained plateau) by approximately 50% above basal rates but did not alter the rate of glucose uptake. Thus, our data clearly demonstrate that the sustained plateau component of the CT response arises from an increased rate of glycolysis, leading to efflux of lactic acid, which may be mediated by a member of the family of monocarboxylate transporters. A recent study demonstrated that activation of heterologously expressed human CTRs leads to gradual acidification of the culture medium over a period of 1–3 d (28). Additionally, it has been shown that CT transiently increases proton efflux from neonatal mouse calvariae (29). However, the mechanisms underlying these effects were not characterized in either study.

Signal transduction pathways mediating CT-induced proton efflux from C1a cells

The C1a receptor couples through multiple G proteins to modulate the adenylyl cyclase/PKA pathway and the

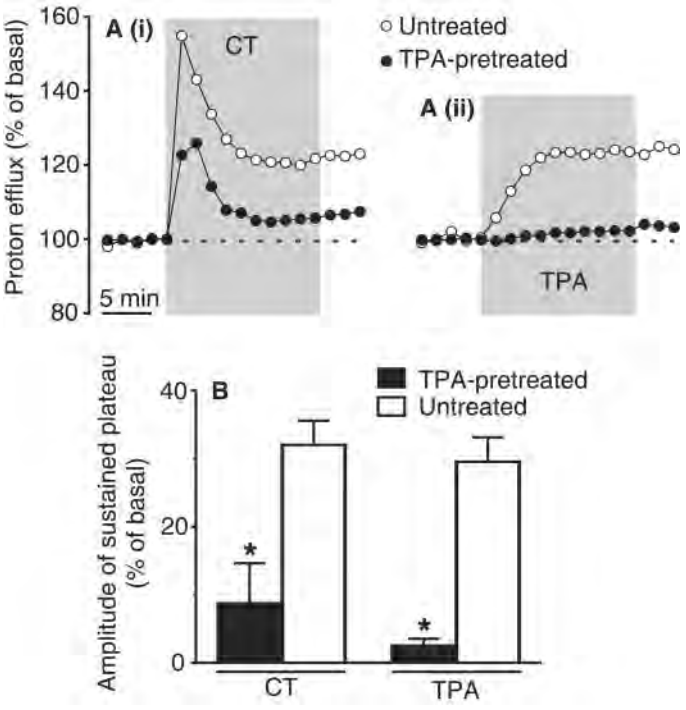

FIG. 12. Effect of chronic pretreatment with TPA on proton efflux. C1a cells were incubated with TPA (100 nM, 16 h) in serum-free α-MEM to deplete protein kinase C. TPA-pretreated and untreated cells were then superfused with standard medium, and proton efflux was monitored using microphysiometry. Where indicated by the *shaded areas*, parallel samples were superfused with CT [10 nM, A (i)] or TPA [100 nM, A (ii)]. B, *Bars* represent the amplitudes of the sustained plateau induced by CT or TPA. Data are changes in proton efflux above basal expressed as percentage of basal efflux (means ± SE of three to six samples from two to three separate cell preparations); *, $P < 0.05$ for the effect of TPA pretreatment. Mean values of basal proton efflux per sample were (in nmol proton equivalents/min): 0.17 ± 0.04 for untreated (n = 9) and 0.27 ± 0.05 for TPA-pretreated (n = 9).

PLC/Ca^{2+}/PKC pathway. In contrast, the CTRΔe13 isoform couples to the adenylyl cyclase/PKA pathway but not to the PLC/Ca^{2+}/PKC pathway. It is possible that CT-induced activation of Na^+/H^+ exchange in C1a cells is mediated by the α-subunit of a heterotrimeric G protein activated by C1a, but not CTRΔe13, as shown for $G\alpha_q$ and $G\alpha 13$ in other systems (17). Second-messenger-dependent signaling pathways may mediate the effects of CT on glycolysis and Na^+/H^+ exchange. The lack of effect of CT on proton efflux from CTRΔe13 cells indicates that cAMP-dependent pathways do not mediate an increase in proton efflux. This was further confirmed by the small response to the cAMP analog CPT-cAMP and the inability of the phosphodiesterase inhibitor IBMX to potentiate CT responses in C1a cells.

Elevation of $[Ca^{2+}]_i$ activates NHE-1 in certain systems via a Ca^{2+}/calmodulin site on the exchanger (17). In our study, the EC_{50} for the effect of CT on proton efflux was markedly less than its EC_{50} for elevation of $[Ca^{2+}]_i$, indicating that if Ca^{2+} were to induce proton efflux, only small elevations of $[Ca^{2+}]_i$ would be required to elicit the response. However, the Ca^{2+} ionophore, ionomycin, and the SERCA inhibitor thapsigargin suppressed proton efflux, in spite of causing elevations in $[Ca^{2+}]_i$ similar to those induced by CT. Moreover, the response to CT was still observed in cells loaded with the intracellular Ca^{2+} chelator BAPTA. Thus, CT-induced elevation of $[Ca^{2+}]_i$ does not stimulate proton efflux from C1a cells.

PKC-mediated activation of proton production and efflux has been reported in other systems (22–24, 30–32). Several observations indicate that PKC underlies at least part of the sustained plateau phase of the CT response in C1a cells. First, TPA [a potent activator of the conventional and novel PKC isoforms (α, βI, βII, γ, δ, ϵ, η, and θ)] causes a sustained glucose-dependent increase in proton and lactate efflux, mimicking the plateau phase of the CT-response. Second, in cells treated chronically with TPA to deplete PKC, the sustained plateau phase of the CT response is markedly suppressed. Third, in cells treated acutely with TPA, CT evokes only a transient increase in proton efflux, without further increase in the plateau phase. Fourth, in C1a cells previously treated with CT, TPA fails to elicit any further increase in proton efflux. Thus, activation of PKC seems to underlie the sustained plateau phase of the response to CT. An alternative explanation is that TPA leads to desensitization of the CTR via PKC-mediated phosphorylation. However, this is unlikely because cells treated with TPA (acutely or chronically) still responded to CT with a transient increase in proton efflux (Figs. 9A and 12Ai). Furthermore, CT induces full elevation of $[Ca^{2+}]_i$ in cells acutely treated with TPA (data not shown). Our findings are in keeping with previous reports showing that activation of PKC stimulates 6-phosphofructo-2-kinase activity, glycolysis, and lactate production in hepatocytes and fibroblasts (23, 24). It is possible that the sustained plateau phase of the CT response is mediated by either Ca^{2+}-sensitive or -insensitive PKC isoforms, because chelating cytosolic Ca^{2+} with BAPTA does not reduce basal $[Ca^{2+}]_i$ in C1a cells (134 ± 19 nM in control cells *vs.* 186 ± 12 nM in BAPTA-loaded cells, n = 7). In this regard, both CT and TPA activate PKCα (a Ca^{2+}-sensitive conventional PKC isoform) in a porcine renal tubule cell line that possesses native CTRs (33).

The kinase inhibitor staurosporine and the more specific PKC inhibitor bisindolylmaleimide I partially inhibit the effects of CT on proton efflux. At the concentration used in our studies, staurosporine inhibits PKC (isoforms α, βI, βII, γ, δ, and ϵ), PKA, protein kinase G, CaM kinase, and myosin light chain kinase. Staurosporine partially inhibited both the initial transient and the sustained plateau of the CT response. On the other hand, bisindolylmaleimide I, a more potent and selective inhibitor of PKC (isoforms α, βI, βII, γ, δ, and ϵ), primarily inhibited the plateau phase. These findings establish that a PKC-dependent pathway underlies, at least in part, the sustained plateau phase of the CT response. Though bisindolylmaleimide completely blocks the effects of TPA on proton efflux from C1a cells, it only partially inhibits the CT response, suggesting that, in addition to PKC, an as-yet-unidentified mechanism is also involved.

Possible physiological significance of the effects of CT on proton efflux

CT regulates Ca^{2+} homeostasis by inhibiting osteoclastic bone resorption and enhancing renal Ca^{2+} excretion. Expression of the C1a and CTRΔe13 CTR isoforms varies in a tissue-specific manner, with CTRΔe13 accounting for 10–15% in osteoclasts, kidney, and brain and at least 50% in skeletal muscle and lung (10). The differences in expression pattern and signaling between the two isoforms may be involved in regulation of CT actions. In bone and kidney, ion transport processes play major roles in skeletal remodeling, maintenance of cellular volume, transepithelial transport, and calcium and acid-base homeostasis. Secretion of proton equivalents into the renal tubular lumen is mediated by two transporters, the Na^+/H^+ exchanger and H^+-ATPase (34). Activation of Na^+/H^+ exchange may play a role in the regulation by CT of both Na^+ reabsorption and proton secretion in the kidney. In osteoclasts, activation of the basolateral Na^+/H^+ exchanger may decrease the availability of protons for the ruffled border (apical) vacuolar H^+-ATPase, thus rapidly diminishing resorptive activity.

In conclusion, we report, for the first time, that CT acts selectively through the C1a receptor isoform to activate a biphasic increase in proton efflux. Na^+/H^+ exchange mediates the initial transient, whereas glucose-dependent metabolic acid production is responsible for the sustained plateau phase. Activation of PKC underlies the sustained plateau phase of the response to CT.

Acknowledgments

We thank Ms. Elizabeth Pruski for expert technical assistance with cell culture and lactate assays, Dr. Svetlana V. Komarova and Dr. Stephen M. Sims (Department of Physiology, University of Western Ontario) for helpful comments and advice, and Dr. Udo Albus (Aventis Pharma, Germany) for providing cariporide.

Received February 23, 2001. Accepted June 11, 2001.

Address all correspondence and requests for reprints to: Dr. S. J. Dixon, Department of Physiology, Faculty of Medicine and Dentistry, The University of Western Ontario, London, Ontario, Canada N6A 5C1. E-mail: jeff.dixon@fmd.uwo.ca.

This work was supported by the Canadian Institutes of Health Research [Grant MOP-10854 (to S.J.D.) and Studentship Award (to A.S.)] and by National Institutes of Health [Grant DE-04724 (to R.B.)]. P.C. is a Research Scholar of the Heart and Stroke Foundation of Canada. A preliminary report of this work has appeared in the abstracts of the American Society for Bone and Mineral Research, 2000.

References

1. **Azria M, Copp D, Zanelli J** 1995 25 years of salmon calcitonin: from synthesis to therapeutic use. Calcif Tissue Int 57:405–408
2. **Hoff A, Thomas P, Cote C, et al.** 1998 Generation of a calcitonin knockout mouse model. Bone 23:S164 (Abstract)
3. **Sexton P, Findlay D, Martin T** 1999 Calcitonin. Curr Med Chem 6:1067–1093
4. **Lin H, Harris T, Flannery M, et al.** 1991 Expression cloning of an adenylate cyclase-coupled calcitonin receptor. Science 254:1022–1024
5. **Gorn A, Lin H, Yamin M, et al.** 1992 Cloning, characterization, and expression of a human calcitonin receptor from an ovarian carcinoma cell line. J Clin Invest 90:1726–1735
6. **Yamin M, Gorn A, Flannery M, et al.** 1994 Cloning and characterization of a mouse brain calcitonin receptor complementary deoxyribonucleic acid and mapping of the calcitonin receptor gene. Endocrinology 135:2635–2643
7. **Kuestner R, Elrod R, Grant F, et al.** 1994 Cloning and characterization of an abundant subtype of the human calcitonin receptor. Mol Pharmacol 46: 246–255
8. **Albrandt K, Mull E, Brady E, Herich J, Moore C, Beaumont K** 1993 Molecular cloning of two receptors from rat brain with high affinity for salmon calcitonin. FEBS Lett 325:225–232
9. **Sexton P, Houssami S, Hilton J, et al.** 1993 Identification of brain isoforms of the rat calcitonin receptor. Mol Endocrinol 7:815–821
10. **Shyu J, Inoue D, Baron R, Horne W** 1996 The deletion of 14 amino acids in the seventh transmembrane domain of a naturally occurring calcitonin receptor isoform alters ligand binding and selectively abolishes coupling to phospholipase C. J Biol Chem 271:31127–31134
11. **Zaidi M, Datta H, Moonga B, MacIntyre I** 1990 Evidence that the action of calcitonin on rat osteoclasts is mediated by two G proteins acting via separate post-receptor pathways. J Endocrinol 126:473–481
12. **Shyu JF, Zhang Z, Hernandez-Lagunas L, et al.** 1999 Protein kinase C antagonizes pertussis-toxin-sensitive coupling of the calcitonin receptor to adenylyl cyclase. Eur J Biochem 262:95–101
13. **Chen Y, Shyu J, Santhanagopal A, et al.** 1998 The calcitonin receptor stimulates Shc tyrosine phosphorylation and Erk1/2 activation: involvement of Gi, protein kinase C, and calcium. J Biol Chem 273:19809–19816
14. **McConnell H, Owicki J, Parce J, et al.** 1992 The cytosensor microphysiometer: biological applications of silicon technology. Science 257:1906–1912
15. **Grynkiewicz G, Poenie M, Tsien R** 1985 A new generation of Ca^{2+} indicators with greatly improved fluorescence properties. J Biol Chem 260:3440–3450
16. **Santhanagopal A, Dixon S** 1999 Insulin-like growth factor I rapidly enhances acid efflux from osteoblastic cells. Am J Physiol 277:E423–E432
17. **Wakabayashi S, Shigekawa M, Pouyssegur J** 1997 Molecular physiology of vertebrate Na^+/H^+ exchangers. Physiol Rev 77:51–74
18. **Szabo E, Numata M, Shull G, Orlowski J** 2000 Kinetic and pharmacological properties of human brain Na^+/H^+ exchanger isoform 5 stably expressed in Chinese hamster ovary cells. J Biol Chem 275:6302–6307
19. **Scholz W, Albus U, Counillon L, et al.** 1995 Protective effects of HOE642, a selective sodium-hydrogen exchange subtype 1 inhibitor, on cardiac ischaemia and reperfusion. Cardiovasc Res 29:260–268
20. **Siga E, Houillier P, Mandon B, Moine G, de Rouffignac C** 1996 Calcitonin stimulates H^+ secretion in rat kidney intercalated cells. Am J Physiol 271: F1217–F1223
21. **Moolenaar W** 2000 Development of our current understanding of bioactive lysophospholipids. Ann NY Acad Sci 905:1–10
22. **Gupta A, Schwiening C, Boron W** 1994 Effects of CGRP, forskolin, PMA, and ionomycin on pHi dependence of Na-H exchange in UMR-106 cells. Am J Physiol 266:C1088–C1092
23. **Meacci E, Vasta V, Vannini F, Farnararo M, Bruni P** 1994 Bradykinin stimulates fructose 2,6-bisphosphate metabolism in human fibroblasts. Biochim Biophys Acta 1221:233–237
24. **Conricode K, Ochs R** 1990 Epidermal growth factor and 12-*O*-tetradecanoylphorbol 13-acetate stimulate lactate production and the pentose phosphate pathway in freshly isolated rat hepatocytes. J Biol Chem 265:20931–20937
25. **Lamp S, Findlay D, Moseley J, Martin T** 1981 Calcitonin induction of a persistent activated state of adenylate cyclase in human breast cancer cells (T 47D). J Biol Chem 256:12269–12274
26. **Schneider H, Raue F, Zink A, Koppold A, Ziegler R** 1988 Down-regulation of calcitonin receptors in T47D cells by internalization of calcitonin-receptor complexes. Mol Cell Endocrinol 58:9–15
27. **Dagher G, Thomas S, Griffiths N, Siaume-Perez S, Sauterey C** 1997 Calcitonin activates an Na^+-independent HCO_3^--dependent pathway in the rabbit distal convoluted tubule. Am J Physiol 273:F97–F103
28. **Raggatt L-J, Evdokiou A, Findlay D** 2000 Sustained activation of Erk1/2 MAPK and cell growth suppression by the insert-negative, but not the insert-positive isoform of the human calcitonin receptor. J Endocrinol 167:93–105
29. **Belinsky G, Tashjian AJ** 2000 Direct measurement of hormone-induced acidification in intact bone. J Bone Miner Res 15:550–556
30. **Baxter G, Miller D, Kuo R, Wada H, Owicki J** 1992 PKC epsilon is involved in granulocyte-macrophage colony-stimulating factor signal transduction: evidence from microphysiometry and antisense oligonucleotide experiments. Biochemistry 31:10950–10954
31. **Wada H, Indelicato S, Meyer L, et al.** 1993 GM-CSF triggers a rapid, glucose dependent extracellular acidification by TF-1 cells: evidence for sodium/proton antiporter and PKC mediated activation of acid production. J Cell Physiol 154:129–138
32. **Pitchford S, De Moor K, Glaeser B** 1995 Nerve growth factor stimulates rapid metabolic responses in PC12 cells. Am J Physiol 268:C936–C943
33. **Naro F, Perez M, Migliaccio S, et al.** 1998 Phospholipase D- and protein kinase C isoenzyme-dependent signal transduction pathways activated by the calcitonin receptor. Endocrinology 139:3241–3248
34. **Capasso G, Saviano C, Rizzo M, et al.** 1997 Update on renal acidification: a physiological view. Miner Electrolyte Metab 23:243–248